ELSEVIER

ISPRS Journal of Photogrammetry & Remote Sensing 54 (1999) 68–82

PHOTOGRAMMETRY & REMOTE SENSING

Airborne laser scanning—an introduction and overview

Aloysius Wehr [a,*], Uwe Lohr [b]

[a] *Institute for Navigation, University of Stuttgart, Geschwister-Scholl-Str. 24D, D-70174 Stuttgart, Germany*
[b] *TopoSys, Freiherr-v.-Stein-Str. 7, D-88212 Ravensburg, Germany*

Received 22 December 1998; accepted 24 March 1999

Abstract

This tutorial paper gives an introduction and overview of various topics related to airborne laser scanning (ALS) as used to measure range to and reflectance of objects on the earth surface. After a short introduction, the basic principles of laser, the two main classes, i.e., pulse and continuous-wave lasers, and relations with respect to time-of-flight, range, resolution, and precision are presented. The main laser components and the role of the laser wavelength, including eye safety considerations, are explained. Different scanning mechanisms and the integration of laser with GPS and INS for position and orientation determination are presented. The data processing chain for producing digital terrain and surface models is outlined. Finally, a short overview of applications is given.

Keywords: airborne laser scanning; pulse lasers; CW-lasers; laser ranging resolution and precision; laser scanning methods; position and orientation systems; airborne laser scanning (data processing chain)

1. Introduction

Before going into details of different laser scanning systems, the term laser scanning shall be defined. Laser scanners utilise opto-mechanical scanning assemblies just as many multispectral scanners like the spaceborne scanner on Skylab, the LANDSAT MSS and the Thematic Mapper TM. However, they are active sensing systems using a laser beam as the sensing carrier. Therefore, two optical beams—the emitted laser beam and the received portion of that beam—must be considered. All laser systems measure by some means the distance between the sensor and the illuminated spot on ground. As shown in Fig. 1, a typical laser scanner can be subdivided into the following key units: laser ranging unit, opto-mechanical scanner, control and processing unit. The ranging unit comprises the emitting laser and the electro-optical receiver. The transmitting and receiving apertures (typically 8–15 cm diameter) are mounted so that the transmitting and receiving paths share the same optical path. This assures that object surface points illuminated by the laser are always in the field of view (FOV) of the optical receiver. The narrow divergence of the laser beam defines the instantaneous field of view (IFOV). Typically, the IFOV ranges from 0.3 mrad to 2 mrad. The theoretical physical limit of the IFOV is determined by diffraction of light, which causes image blurring. Therefore, the IFOV is a function of the transmitting

* Corresponding author. E-mail: aloysius.wehr.@nav.uni-stuttgart.de

0924-2716/99/$ - see front matter
PII: S0924-2716(99)00011-8

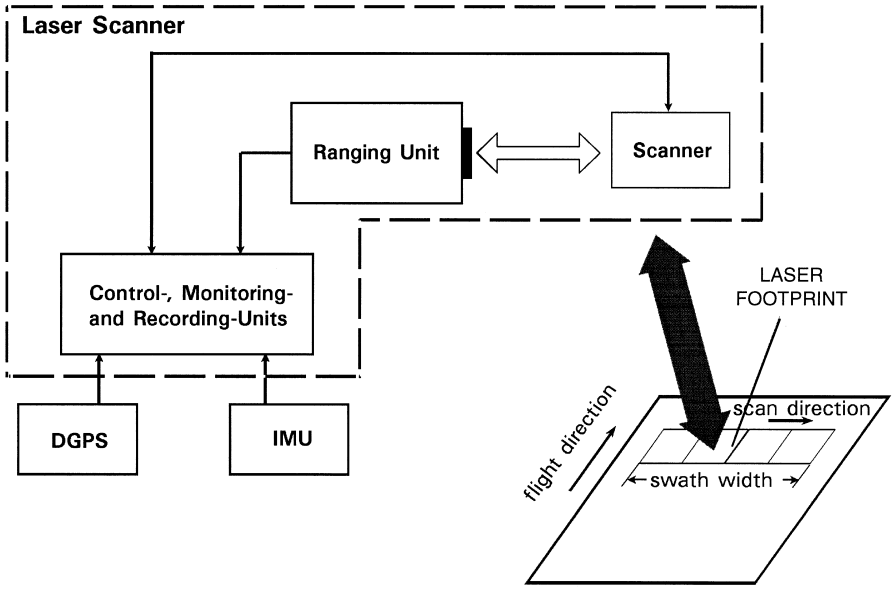

Fig. 1. A typical ALS system.

aperture D and the wavelength of the laser light λ. For spatially coherent light, the diffraction-limited IFOV is given by:

$$\mathrm{IFOV}_{\mathrm{diff}} = 2.44\frac{\lambda}{D}. \quad (1)$$

The IFOV of the receiving optics must not be smaller than that of the transmitted laser beam. Due to the very narrow IFOV of the laser, the optical beam has to be moved across the flight direction in order to obtain area coverage required for surveying. The second dimension is realised by the forward motion of the airplane (see Fig. 1). Thus, laser scanning means deflecting a ranging beam in a certain pattern so that an object surface is sampled with a high point density.

In the following, first a closer look will be taken to laser ranging and opto-mechanical scanners. Then, the total laser scanner system will be introduced, consisting of the laser scanner, a position and orientation system (POS), realised by an integrated differential GPS (DGPS) and an inertial measurement unit (IMU), and the control unit. There, the synchronisation problem will also be considered. The processing steps for obtaining digital elevation models (DTM), digital surface models (DSM) and digital city models will be presented. Finally, a short overview of applications is given.

2. Laser ranging

In contrast to microwave radar technique, lasers are of advantage for range measurements as, on the one hand, high energy pulses can be realised in short intervals and on the other hand, their comparatively short wavelength light can be highly collimated using small apertures (see Eq. (1)). For these reasons, already shortly after the advent of lasers, very precise ranging was carried out with this new tool. As soon as lasers with high pulse repetition rates were available on the market, scanning laser systems could be realised with the ability to obtain range images. Such systems are also known as laser radar. For laser radar, two acronyms are commonly used LADAR (*LA*ser *D*etection *A*nd *R*anging) and LIDAR (*LI*ght *D*etection *A*nd *R*anging) (Bachman, 1979, p. 2 and Jelalian, 1992, p. 1). An official terminology does not exist. The authors prefer LADAR because this expression makes clear that a laser is used. Laser light is very special. The acronym laser stands for *l*ight *a*mplification by *s*timulated *e*mission of *r*adia-

tion. Young (1986), (p. 145) explains that using this process, a powerful highly directional optical light beam can be generated which is often very highly coherent both in space and time. The level of coherence is very dependent on the laser. Gas and solid-state lasers offer higher coherence than semiconductor lasers. However, in current laser scanning, the physical effect of coherence is of no relevance. Only the high collimation and the high optical power of lasers are required. A LIDAR may also be built up by xenon or flash lamps, which are no laser sources.

In range measurements with laser, two major ranging principles are applied: the pulsed ranging principle, and ranging by measuring the phase difference between the transmitted and the received signal backscattered from the object surface. The phase difference method is applied with lasers that continuously emit light. These lasers are called continuous wave (CW) lasers.

In current ranging laser systems, mostly pulsed lasers are used. Pulse lasers are usually solid-state lasers, which produce high power output. They can be pumped with light from xenon flash tubes, arc lamps, metal–vapour lamps and laser diodes, which are especially applied for pumping airborne lasers. A common type is the Nd:YAG laser, with pulse widths of 10–15 ns, 1.06 μm wavelength and peak power up to several MW. There is only one CW-laser scanner, employed in commercial airborne laser scanning (ALS), which was developed and realised by the Institute of Navigation, University of Stuttgart. In the following, the ranging principles will be introduced and the performance of pulsed and CW-lasers scanners will be discussed. It will be shown that both principles measure the travelling time of a signal—however, different physical effects are utilised.

2.1. Pulse and CW ranging

Fig. 2 shows a typical ranging set-up. The most direct ranging measurement is determining the time-of-flight of a light pulse, i.e., by measuring the travelling time between the emitted and received pulse (see Fig. 3). According to Fig. 3, the travelling time of a light pulse is:

$$t_L = 2\frac{R}{c} \tag{2}$$

with R the distance between the ranging unit and the object surface and c the speed of light. From Eq. (2),

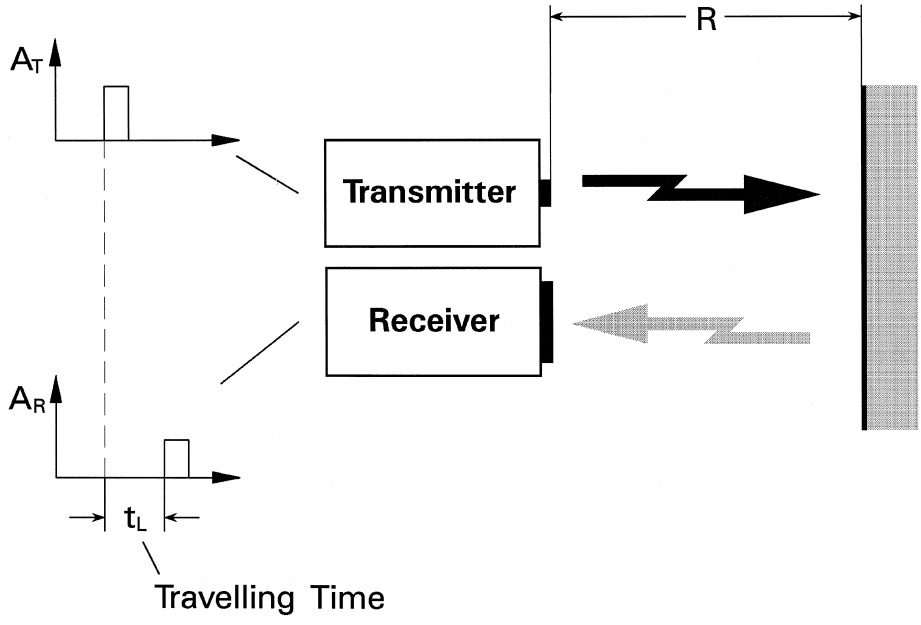

Fig. 2. Time-of-flight ranging. A_T and A_R are the transmitted and received amplitudes, respectively.

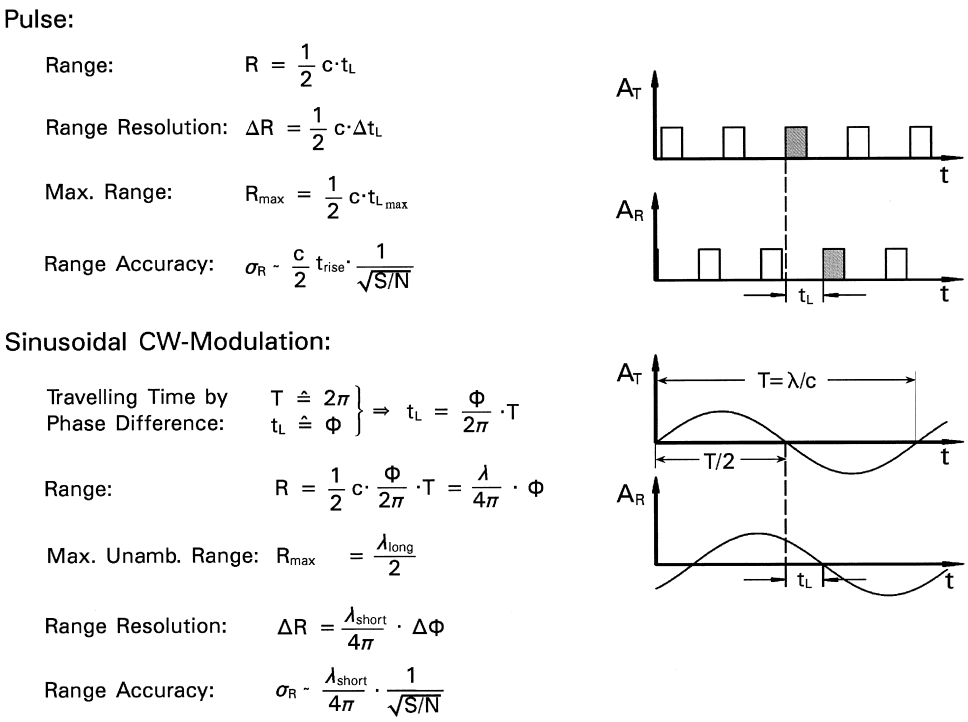

Fig. 3. Measuring principle of pulse and CW-lasers. On the right, the first and third figures show the transmitted signal, the second and fourth figures the received one. A_T and A_R are the amplitudes of the transmitted and received signal, respectively.

the range resolution ΔR, which is directly proportional to the time resolution Δt_L, can be derived:

$$\Delta R = \frac{1}{2} c \Delta t_L . \tag{3}$$

If the laser transmits a continuous signal, ranging can be carried out by e.g., modulating the light intensity of the laser light with e.g., a sinusoidal signal (see Fig. 3). Fig. 3 shows that the sinusoidal signal is received with a time delay t_L, as for the pulse laser. However, the period T of the signal is known and therefore, the travelling time t_L is directly proportional to the phase difference ϕ between the received and transmitted signal. t_L is calculated by:

$$t_L = \frac{\phi}{2\pi} T + nT \tag{4}$$

with n the number of full wavelengths included in the distance from laser transceiver to receiver. In the following Eqs. (5) and (6) and the respective equations in Fig. 3, the contribution of the full periods and wavelengths to travelling time and range, respectively will be ignored. As the period T of the ranging signal is inversely proportional to its frequency f, the travelling time can be written as:

$$t_L = \frac{\phi}{2\pi} \frac{1}{f} \tag{5}$$

If the phase difference is measured, the range is determined by:

$$R = \frac{1}{4\pi} \frac{c}{f} \phi \tag{6}$$

Analogously to pulse ranging, the range resolution is given by:

$$\Delta R = \frac{1}{4\pi} \frac{c}{f} \Delta\phi . \tag{7}$$

Comparing Eqs. (3) and (7), it becomes clear that using pulse systems, the resolution is determined by the resolution of the time interval measurement. However, using CW-systems, one additional physi-

cal parameter (i.e., f) is obtained. The frequency f of the actual ranging signal determines the ranging sensitivity. Eq. (7) shows that by the increasing frequency f, higher range resolution (lower ΔR) can be achieved for a given phase resolution.

The advantages and disadvantages of both measurement principles will be now discussed (see also Fig. 3). The maximum measurable phase difference is 360°. For angles greater than 360°, the modulo 2π of the phase difference angle is used. Therefore, with regard to Eq. (6), the maximum unambiguous range for $\phi_{\max} = 2\pi$ is:

$$R_{\max} = \frac{1}{4\pi}\frac{c}{f}\phi = \frac{1}{4\pi}\lambda\phi = \frac{\lambda}{2} \qquad (8)$$

with λ the wavelength of the actual ranging signal (in CW-lasers with multiple frequencies λ_{long}, see below). In general, for CW-laser ranging system several frequencies (tones) must be applied to achieve high resolution and long maximum unambiguous range $R_{\max}$. If a multifrequency system is used, the frequency with the longest wavelength λ_{long} determines $R_{\max}$ (see Eq. (8)) and the frequency with the shortest wavelength λ_{short} determines the range resolution and accuracy. Using pulses, the maximum range is only limited by the maximum time interval, which can be measured by the time counter of the laser (see equation in Fig. 3). However, in practise, this time interval is large enough, so that the maximum range is rather limited due to laser energy losses during travel and other factors.

Besides $R_{\max}$, the ranging accuracy σ is a key parameter. According to the equations in Fig. 3, ranging accuracy depends on the ranging signal, which is described by the pulse length or the rise time for pulse ranging, and the wavelength of the ranging tone for CW-laser ranging. Furthermore, the ranging accuracy is inversely proportional to the square root of the signal-to-noise ratio (S/N). The S/N depends on many factors, as power of received signal, input bandwidth (measurement rate), background radiation, responsivity of the signal detector (usually PIN- or avalanche photodiode), amplifier noise, etc., whereby some of the previous factors again depend on other parameters, e.g., the received power depends on the transmitted power, aperture of receiving optics, target range, etc. Fig. 4 shows the relations between different parameters, and their influence on S/N and range accuracy. If the optical power of the received signal is so low that only

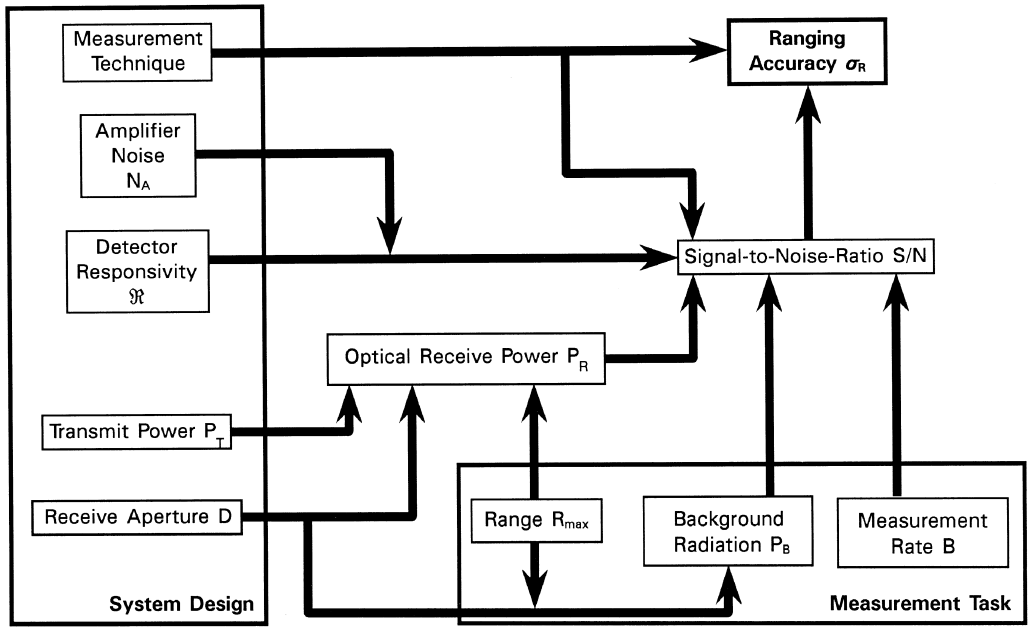

Fig. 4. Relations between different parameters and their influence on S/N and range accuracy.

thermal noise (no shot noise) contributes to the noise term, the S/N can be simplified to:

$$S/N = \frac{\text{signal power of the photodiode current}}{\text{thermal noise power of the photodiode and amplifier}}. \quad (9)$$

In this case, the square root of S/N is directly proportional to the received optical power P_R. The noise input bandwidths B_{pulse} and B_{CW} below (for pulse ranging systems and phase difference measurements) are inversely proportional to the pulse rise time t_{rise} and proportional to the measurement rate, respectively. For the ranging accuracy, the following proportionalities can be defined:

Pulse ranging:

$$\sigma_{R_{pulse}} \sim \frac{c}{2} t_{rise} \frac{\sqrt{B_{pulse}}}{P_{R_{peak}}} \quad (10)$$

CW-ranging:

$$\sigma_{R_{CW}} \sim \frac{\lambda_{short}}{4\pi} \frac{\sqrt{B_{CW}}}{P_{R_{av}}} \quad (11)$$

with $P_{R_{peak}}$ the received peak optical power and $P_{R_{av}}$ the received average optical power.

To compare the performance of both measurement principles, it is assumed that the same target is illuminated. In this case, the received optical power can be replaced by the transmitted optical power, which is the peak power $P_{T_{peak}}$ of the laser pulse for pulse systems and the average emitted optical power $P_{T_{av}}$ for CW-systems, respectively. The ratio of accuracies is then proportional according to

$$\frac{\sigma_{R_{pulse}}}{\sigma_{R_{CW}}} \sim 2\pi \frac{c}{\lambda} t_{rise} \frac{P_{T_{av}}}{P_{T_{peak}}} \sqrt{\frac{B_{pulse}}{B_{CW}}} \quad (12)$$

or

$$\frac{\sigma_{R_{pulse}}}{\sigma_{R_{CW}}} \sim 2\pi f \sqrt{\frac{t_{rise}}{B_{CW}}} \frac{P_{T_{av}}}{P_{T_{peak}}} \quad (13)$$

Eq. (13) is derived from Eq. (12) with the assumption that:

$$t_{rise} \sim \frac{1}{B_{pulse}} \quad (14)$$

Assuming a 1 ns pulse rise time and a transmitted peak power of 2000 W for the pulse system and a ranging tone of 10 MHz, a bandwidth B_{CW} (corresponding to the measurement rate) of 7 kHz and an average transmitted power of 1 W for the CW-laser system, the ratio $\sigma_{R_{pulse}}/\sigma_{R_{CW}}$ is proportional to 0.012. This means that the pulse system may theoretically achieve an 85 times higher accuracy than the CW one, although with a 2000 times higher peak power. For the pulse system, an average transmitting power $P_{T_{av}}$ can be calculated by:

$$P_{T_{av}} = P_{T_{peak}} t_p \text{PRF} \quad (15)$$

with t_p the pulse duration (usually around 10 ns for ALS) and PRF the pulse repetition frequency (pulse rate, measurement rate). Assuming a PRF of 10 kHz, the average power for a pulse system is 0.2 W, i.e., in the range of the average power of the CW-lasers. This system analysis and the calculations carried out by Wehr (1994a,b) show that the laser power is essential, if ranging is carried out to non-cooperative targets. The fact that pulse lasers with high energy are available on the market, while semiconductor CW-lasers with direct modulation capabilities of up to 10 MHz and more than 2 W can hardly be found, explains why commercial laser range finders work with pulse ranging units. The performed calculations are only valid as far as ranging accuracies in the centimeter level are concerned. With regard to pulse systems, achieving higher accuracy requires very high technical efforts and sophisticated processing methods. Sub-centimeter level accuracy can be achieved easily with CW-systems by using a higher frequency, although the phase difference measurement electronics remain the same.

2.2. Lasers

In current ranging ALS, semiconductor diode lasers and Nd:YAG lasers pumped by semiconductor lasers are used, covering the optical band between 800 nm and 1600 nm. PIN- or avalanche photodiodes (APD) are applied as optical detectors. The sensitivity of the detector is of importance. Under similar conditions, an APD can measure four times the range that can be measured by a PIN-photodiode, and a high-end APD even 10 times the range. As current laser scanners work by the direct energy detection principle, a coherent light source for rang-

Table 1
Typical reflectivity of various diffuse reflecting materials for 900 nm wavelength (modified from the WEB pages of the company Riegl)

Material	Reflectivity (%)
Dimension lumber (pine, clean, dry)	94
Snow	80–90
White masonry	85
Limestone, clay	Up to 75
Deciduous trees	Typ. 60
Coniferous trees	Typ. 30
Carbonate sand (dry)	57
Carbonate sand (wet)	41
Beach sands, bare areas in dessert	Typ. 50
Rough wood pallet (clean)	25
Concrete, smooth	24
Asphalt with pebbles	17
Lava	8
Black neoprene (synthetic rubber)	5

ing is not required. Therefore, the following physical laser properties are used in laser scanning: high power, short pulses or the capability to modulate the laser light with a frequency in case of CW-systems, high collimation, and narrow optical spectrum in which lasers emit. The narrow optical spectrum or in other words, the narrow spectral laser line is advantageous, because narrow optical interference filters (usually with 10 nm bandwidth) can be mounted in the receiving path to suppress disturbing background radiation, caused e.g., by backscattered sunlight.

The selection of the optical wavelength of the laser is dependent on the overall laser scanning system design. The most sensitive detectors are available between 800 nm and 1000 nm. Therefore, the first laser scanners worked with a wavelength of 900 nm. At this wavelength, powerful pulsed semiconductor laser diodes were available on the market and an optimum system performance could be expected. However, at this wavelength of the optical spectrum, eye safety is still a concern. If higher laser pulse energy is required, wavelengths have to be considered in which the eye is less sensitive. The TopoSys laser scanner operates at 1535 nm. At this wavelength, higher energy levels can be used without running the risk to hurt the eye. The higher energy by far compensates the lower sensitivity of InGaAs avalanche photodiodes that are used as detectors at this wavelength. Due to the higher energy, the maximum range can be extended to more than 1500 m maintaining the same ranging performance with respect to S/N and accuracy. In addition, the background radiation caused by the sunlight is very low at 1535 nm. Intensive background radiation degrades the S/N.

When discussing laser wavelength, one should also consider the backscattering properties of the target, e.g., the object surface. Typical diagrams concerning reflection coefficients for e.g., water, sand vegetation can be found in a handbook of Wolfe and Zissis (1978), (Chap. 3). For example, a laser scanner using 1535 nm is not a good choice for measurement of glaciers because snow and ice reflect weakly at 1535 nm. Here, an 810 nm laser may be the better choice. Table 1 shows the typical reflectivity of various materials for 900 nm wavelength.

The reflectivity of a target, for a given wavelength, also influences the maximum range. Thus, specifications of manufacturers, system providers, etc., for the maximum range should always specify for what type of target reflection (diffuse or specular) and percentage of reflectivity, their statement on maximum range is valid. An example of range cor-

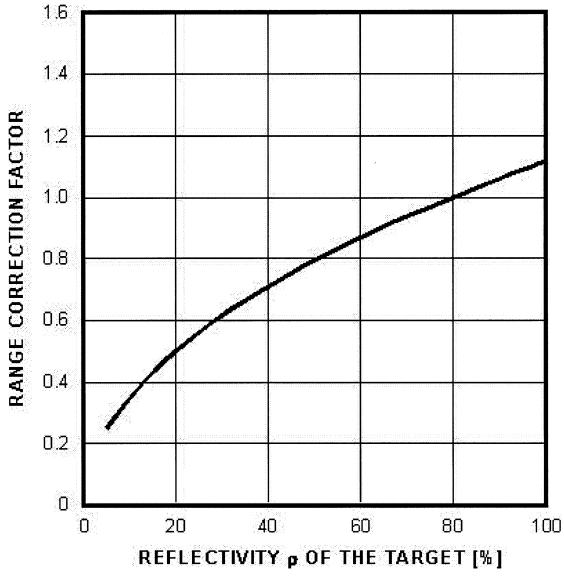

Fig. 5. Correction factor for maximum laser range, depending on target reflectivity (lasers of firm Riegl, 900 nm wavelength, diffuse targets, maximum range in the specifications given for 80% reflectivity).

rection based on target reflectivity for lasers of the firm Riegl (900 nm wavelength, maximum range specifications given for diffuse targets with 80% reflectivity) is shown in Fig. 5. As the figure shows, in that case, targets with 20% and 10% reflectivity have a maximum range of only 50% and 35%, respectively of the one given in the laser specifications.

The laser wavelength, as well as its power, relate to eye safety considerations. Some formulas for estimating the maximum laser power for an eye-safe system are given below. The formulas are derived on the basis of DIN VDE 0837. The area illuminated by the laser A_I (assumed to be circular; the respective circle diameter A_L is also called laser footprint) is given by:

$$A_I = \frac{\pi}{4}(D + R\gamma)^2 \tag{16}$$

with D the aperture of the laser, R the range and γ the angular divergence of the laser beam (γ in this equation is unitless). During flight, one can assume that the eye of an observer is only hit once. For pulse lengths in the range 10 ns $\leq t_p \leq$ 100 ns, the maximum eye-safe peak power P_{peak} is given in Table 2. With respect to the formulas in Table 2, as well as Eqs. (17) and (18), the units are A_I (m^2), t (s), λ (nm), f_{sc} (Hz), and then the left-hand side of the equations (i.e., the power) is given in (W).

If the laser hits the eye repeatedly during scanning, then the maximum eye-safe peak power is calculated by:

$$P_{peak_{sc}} = \frac{P_{peak}}{\sqrt{f_{sc}}} \tag{17}$$

with f_{sc} the scan rate and 1 Hz $< f_{sc} <$ 278 Hz.

Table 2
Maximum eye-safe peak power for different laser wavelengths (pulse laser, single shot)

Wavelength λ (nm)	Peak power
700–1050	$5 \cdot 10^{-3} \cdot 10^{\frac{\lambda - 700}{500}} \frac{1}{t_p} A_I$
1050–1400	$5 \cdot 10^{-2} \frac{1}{t_p} A_I$
> 1400	$100 \frac{1}{t_p} A_I$

For CW-lasers, the maximum eye-safe average power P_{av} is computed for the wavelength range 700 nm–1050 nm by:

$$P_{av} = 18 \cdot 10^{\frac{\lambda - 700}{500}} t^{-0.25} A_I \tag{18}$$

with t exposure duration. This formula can only be applied for exposure times of $1.8 \cdot 10^{-5}$ s to 10^3 s.

3. Scanning

The scanning process was already defined in Section 1. Fig. 1 illustrates the key parameters for a line scan, i.e., the laser footprint and the swath width SW. For a given flying height above ground h, the laser footprint mainly depends on the divergence of the laser beam γ, and the swath width on the scan angle θ, which is also called the FOV. Laser footprint A_L and SW on the ground are given by:

$$A_{L_{inst}} = \frac{h}{\cos^2(\theta_{inst})} \gamma \tag{19}$$

$$SW = 2h \tan\left(\frac{\theta}{2}\right) \tag{20}$$

with $A_{L_{inst}}$ the instantaneous laser footprint and θ_{inst} the instantaneous scan angle with $\theta_{inst} \in [0, \pm \theta/2]$. Besides the parameters A_L and SW, the laser point density is of interest for surveying tasks. The point density is strongly dependent on the used scanner type and the airplane's speed over ground v. Considering e.g., a typical line scan of an oscillating mirror system (see Fig. 1), the point spacing across flight direction dx_{across} mainly depends either on the pulse repetition frequency PRF, if a pulse laser scanner is used or on the measurement rate, if a CW-laser scanner is applied. For the instantaneous dx_{across} one can write:

$$dx_{across_{inst}} = \frac{h}{\cos^2(\theta_{inst})} \frac{\dot{\theta}_{inst}}{PRF} \tag{21}$$

with $\dot{\theta}_{inst}$ the instantaneous angular scanning speed in rad/s. Along flight direction, the point spacing is determined by the speed over ground v of the airplane and the period t_{sc} of one line scan:

$$dx_{along} = v t_{sc}. \tag{22}$$

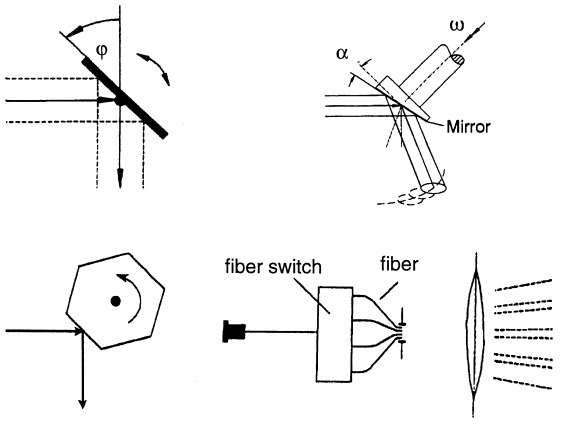

Fig. 6. Scanning mechanisms (from top left, clockwise): oscillating mirror, Palmer scan, fiber scanner, rotating polygon.

Scans can be uni- or bidirectional. Typical scanning mechanisms that are used for airborne surveying are shown in Fig. 6. Oscillating mirrors usually produce a zigzag-line (bidirectional scan) or with two-axis galvanometers a bidirectional meander-type scan of parallel lines or arcs, rotating polygon and multifaceted mirror scanners produce parallel lines (unidirectional scan), nutating mirrors (Palmer scan) produce an elliptical pattern and the fiber scanner produces a parallel line scan. The scan pattern on the ground depends not only on the laser scan pattern but also the flying direction and speed and the terrain topography. The points along a line are usually scanned in equal angle steps, i.e., their spacing on the ground is not constant. Due to acceleration or slow down of the scan mechanism, the points at the swath borders exhibit other characteristics and are sometimes removed from the raw data set.

The advantage of the fiber scanner (used only in the TopoSys system) is that the transmitting and receiving optics are identical (see Fig. 7). An identical fiber line array is mounted in the focal plane of the receiving and transmitting lenses. By means of two rotating mirrors, each fiber in the transmitting and receiving path is scanned sequentially and syn-

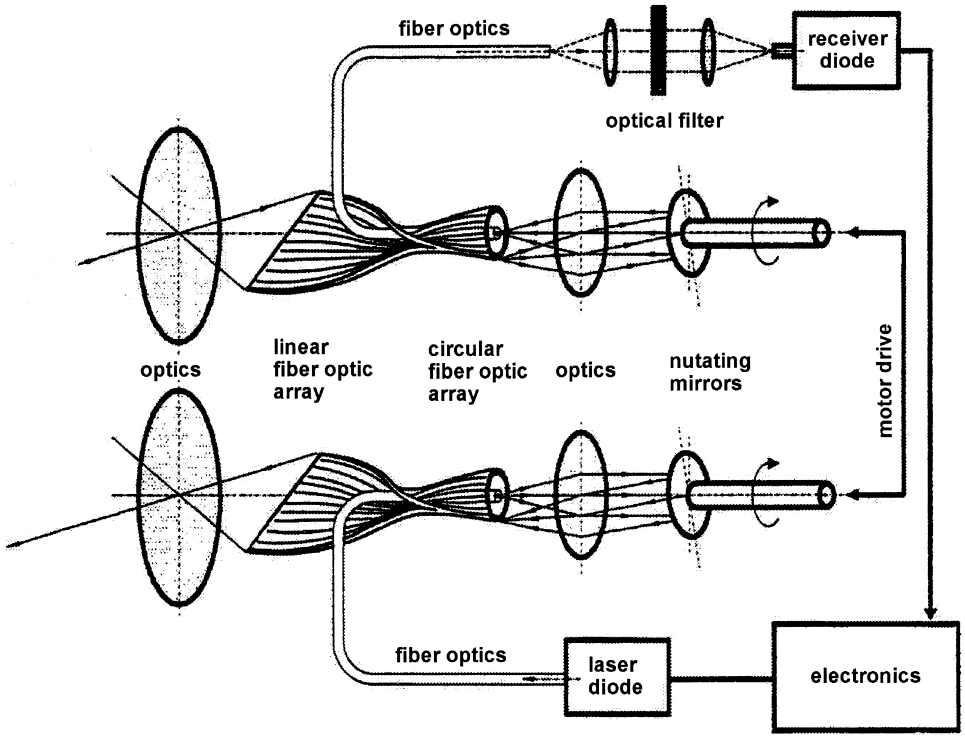

Fig. 7. TopoSys fiber scanner.

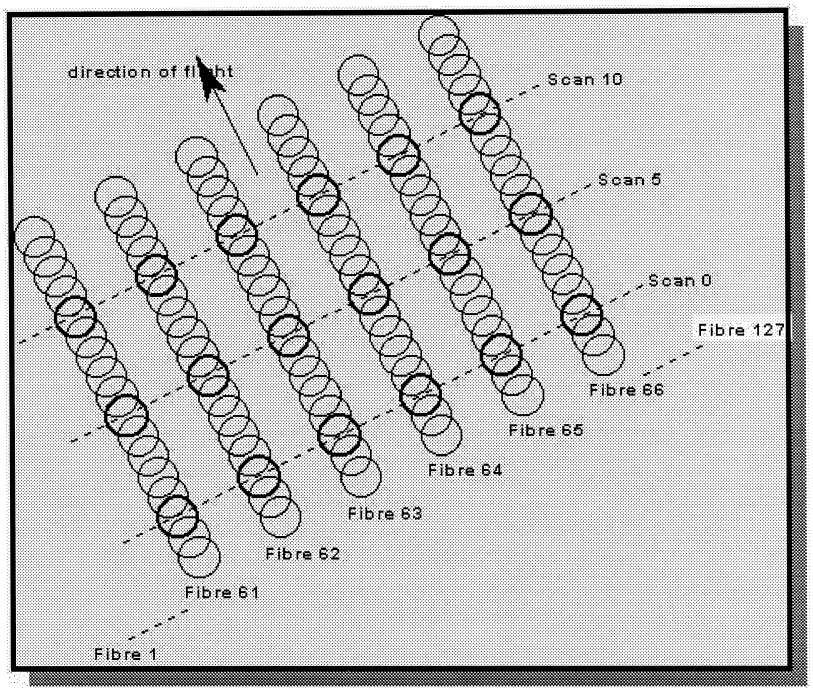

Fig. 8. Scan pattern of TopoSys ALS system.

chronously. These mirrors relay the light either from the central fiber to a fiber of the fiber array mounted in a circle around the central fiber or the other way around from the array to the central fiber. In this way, the light signal from the transmitting fiber is linked to the corresponding fiber in the receiving path. As, due to the small aperture of the fibers, only small moving mechanical parts are required, high scanning speeds (up to 630 Hz) can be achieved. This is not possible with conventional mirror scanners. Up to now, arrays of 128 fibers have been realised, 256 will be possible in the near future. In case of the TopoSys fiber scanner, Eq. (21) cannot be applied without modifications for the across-track point spacing. The across-track spacing of measurements depends on the realised scan angle (here $\pm 7°$

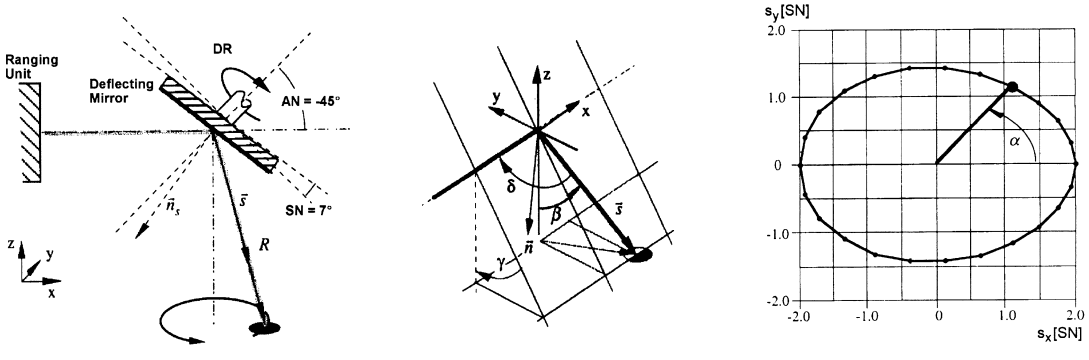

Fig. 9. Palmer scanner: on the left, the scan principle; in the middle, the definition of the direction angles for the laser beam; on the right, the scan pattern and its dimensions.

$= 14°$), the flying altitude h and the number of fibers. For the TopoSys optics geometry, Eq. (21) becomes

$$\mathrm{d}x_{\text{across}} = h\frac{\theta}{N-1} \tag{23}$$

with N the number of fibers and θ in rad. For a flying altitude of 1000 m, $\mathrm{d}x_{\text{across}}$ is equal to 2 m. The along-track resolution depends on the scan rate $(1/t_{\text{sc}})$. In the above case, with a scan rate of 630 Hz and assuming a flying speed of 70 m/s, adjacent scans have a ground distance of 0.11 m. The scan pattern of the TopoSys scanner is shown in Fig. 8. The functioning of the remaining line scanners needs no further explanation.

A very interesting scanning pattern is generated by the Palmer scan (see Fig. 9). The optical beam of the laser ranging unit hits the deflecting mirror, whose rotating axis is mounted so that the scanner shaft and the laser beam form an angle of 45°. In addition, the deflecting mirror is inclined by the angle SN (see Fig. 9). This additional angle causes a nutation of the mirror when the scanner shaft is turning. On ground, an approximately elliptical scanning pattern can be observed. The right plot in Fig. 9 shows the scanning pattern. The coordinates in that plot are in units of the angle SN. To obtain the actual angles, the coordinates must be multiplied by the angle SN. The ellipse translates with the movement of the airplane (see Fig. 10). Due to the elliptical scan, most of the measurement points on ground are scanned twice, once in the forward view and a second time in the backward view. The redundant information on the same ground spot can be favourably used to calibrate the scanner and the POS as far as the pitch angle is concerned.

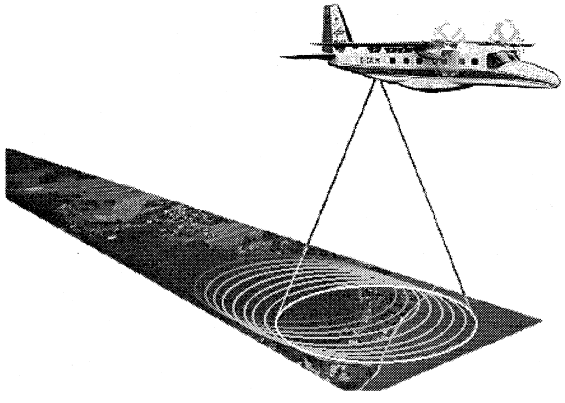

Fig. 10. Progressing Palmer scan.

4. Position and orientation system

The laser scanner measures only the line-of-site vector from the laser scanner aperture to a point on the earth surface. The 3-D position of this point can only be computed, if at any time, the position and orientation of the laser system is known with respect to a coordinate system, e.g., WGS84. Thus, to obtain accurate range measurements in a given coordinate system, a laser scanner system must be supported by a POS. As laser scanners have a potential range accuracy of better than 1 dm, POS should allow at least the same accuracy. Such an accuracy can be achieved only by an integrated POS consisting of a DGPS and an IMU. Geocoding of laser scanner measurements requires an exact synchronisation of all systems: IMU, DGPS and laser scanner data. A possible scheme of time synchronisation is shown in Fig. 11. It illustrates that POS data and laser scanner data are stored on different devices, e.g., hard disks of different PCs. This means that two independent times exist: the GPS time to which POS data are related and the internal time of PC1 to which laser scanner data are related. The objective of the presented scheme is to realise an off-line time synchronisation between laser scanner data and POS data. For this purpose, a software module, which stores the laser scanner data with additional time data controlled by interrupts, is used. At the start of each scan, the local computer time of PC1 is linked into the data stream. In parallel to this recording, the PPS-signal (PPS = pulse per second) of GPS and the local time of PC1 are stored in a separate protocol file. As the PPS-signal of the onboard GPS receiver triggers the interrupt IRQ7, the GPS-time and local time of PC1 are stored at the same instant. Using this protocol file, the POS data can be pre-processed separately from the laser scanner data. The synchronisation on the basis of 1-s time intervals enables the determination and correction of possible time errors between the highly accurate and stable GPS time and the local computer time of PC1. Time synchronisa-

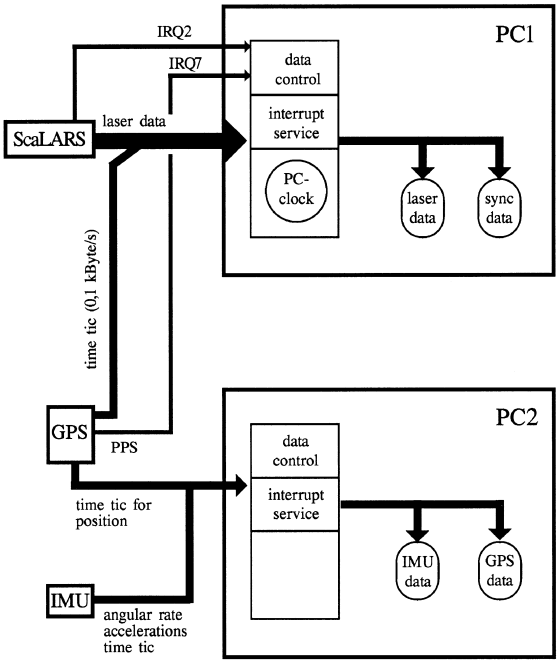

Fig. 11. Synchronisation of laser scanner (ScaLARS), GPS and IMU.

tion of better than 10 μs is achieved operationally by this scheme.

5. Determination of laser points

After a surveying flight, basically two data sets are available: the POS data and the laser ranges with the instantaneous scanning angles (see Fig. 12). Assuming that the accuracy of POS data is better than 1 dm in position and 0.02° in orientation, already very precise laser measurement points in an earth-fixed coordinate system can be calculated. However, some systematic parameters must be considered. These are e.g., the three mounting angles of the laser scanner frame, described by the Euler angles roll, pitch and yaw, with respect to the platform-fixed coordinate system (usually with origin at the IMU), the position of the laser scanner with respect to the IMU, and the position of the IMU with respect to the GPS. This so-called calibration data can be derived from laser scanner surveys, whereby certain reference areas are flown-over in different directions. Reference areas are e.g., flat terrain like large sport fields or stadiums, buildings and corner of buildings. From the relative orientation and position of the different surveys and their absolute orientation and position with respect to an earth-fixed coordinate system, calibration data can be derived. Typical calibration procedures are described by Lindenberger (1993). However, there is no standard procedure. At present, each laser scanning firm has its own procedure for calibration. The experiences of the authors are that these calibration data sets are stable during a survey campaign.

According to Lindenberger (1993) and Hug (1996), laser points in WGS84 can be computed with the help of the three data sets: calibration data and mounting parameters, laser distance measurements with their respective scanning angles and POS data (see Fig. 12). The main objective of the further processing is the calculation of digital elevation models. First, the laser range data must be transformed from WGS84 to the desired local (map) coordinate system. The result is a cloud of randomly distributed laser points in elevation and position. The distribution of the measurement points depends on the scanning pattern of the laser scanner system.

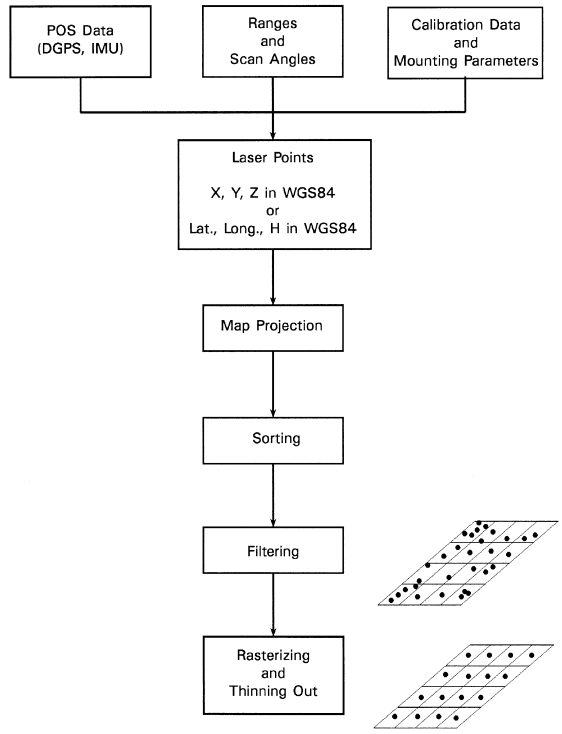

Fig. 12. Typical processing steps for laser scanner data.

Now, the elevation measurements are sorted with respect to their position. After the sorting process, ground points must be separated from non-ground points like buildings and vegetation. For this task, different filter algorithms and procedures are applied. Standard procedures are morphological filtering and the application of autoregressive integrated processes (Lindenberger, 1993). The articles in this issue and the paper of Kraus and Pfeifer (1998) make clear that the development of such filters is not yet completed. This filtering is performed either using the raw data or an interpolated regular grid. The latter has the disadvantage that it is influenced by interpolation errors, but on the other hand, existing filtering methods from image processing can be readily used. Intelligent algorithms were developed for a regular grid DTM interpolation because in most cases several points fall within each grid mesh (Hug and Wehr, 1997). Thus, the interpolation requires certain weighting algorithms. In addition, gaps must be bridged where valid laser measurements are missing, e.g., in thick forest. Since the generated data amount is very high for certain applications and commercial programmes for DTM interpolation, visualisation, etc., can handle only a limited number of points, a thin-out is often applied. This is (or at least should be) performed after filtering and DTM interpolation. Data visualisation and manual editing is necessary in different stages of the processing chain. After studying and comparing measurement results of different laser scanners during the last years, it becomes obvious that the major advancements have been achieved by improvement mainly of the post-processing software and less of the laser scanner hardware. This means that the quality of DTMs, DSMs and city models is very dependent, besides the overall measurement density and the accuracy of the laser scanner system, on the post-processing software.

As the post-processing software determines to a large extent the final result, it is clear that at present, the filtering and interpolation programs are in-house, proprietary programs. Once interpolated, the data can be further processed and analysed by commercial software as e.g., SCOP, Microstation, EASI-PACE and ARC/Info. Currently, the processing time for a DTM computed from laser scanner data is typically three times the data acquisition time.

6. Some extended laser capabilities

Apart from measuring ranges, some lasers can also record the intensity of the backscattered laser

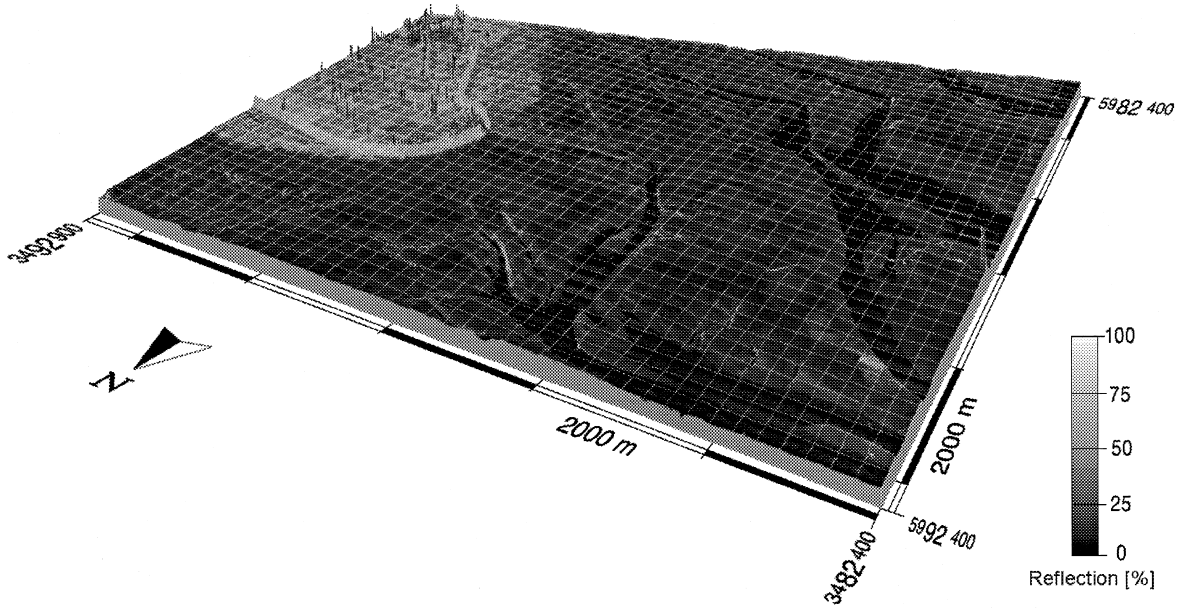

Fig. 13. Intensity data overlaid on DSM (heights multiplied by 50), both produced using the ScarLARS laser scanner. The image shows the shore and shallow of Friedrichskoog, Germany.

light (with intensity measured as the maximum of the returned pulse, or signal integration over the returned pulse width). This can be achieved with both pulse and CW-lasers, although the used principles and the difficulty in their implementation vary. Fig. 13 shows a DSM generated from CW-laser scanner data with laser intensity information. The intensity can be used for visualisation of the scene but also to improve filtering/removal and classification/separation of objects in combination with the range and other information, if available (see for an example, Hug and Wehr, 1997). Some lasers can also record multiple echoes for each pulse sent, i.e., the range (and possibly intensity) of various objects along the pulse path and within the laser footprint. Such systems usually record both the first and last echo of a pulse, although there is one commercial system that can record up to four echoes per pulse. There are also experimental systems that record the whole form of the returned signal (called waveform) with waveform digitisers sampling the incoming signal with very high frequency, e.g., 250 MHz. Lasers that record only one echo, do so for the first or last one (some systems allow switching to first or last, depending on the application). Recording of multiple echoes can be useful, when the vertical profile of multiple objects within the laser footprint (or at least the highest and lowest object), as for example, in the case of trees, is needed. Finally, there are bathymetric lasers, that are based on the same principles as the topographic lasers, but emit in two wavelengths, usually 1064 nm and 532 nm. The infrared wavelength is reflected on the water surface, while the green one penetrates the water and is reflected by the bottom surface or other objects in the water. Commercial systems recording intensity and/or multiple echoes per pulse, as well as bathymetric lasers, are presented in (Baltsavias, 1999).

7. A short overview of applications

Some of the major applications of ALS include:

- Mapping of corridors, e.g., roads, railway tracks, pipelines, waterway landscapes
- Mapping of electrical transmission lines and towers including ground/tree clearance
- DTM generation, especially in forested areas (in forests also for road and path planning, study of drainage patterns, etc.)
- Measurement of coastal areas, including dunes and tidal flats, determination of coastal change and erosion
- High accuracy and very dense measurement applications, e.g., flood mapping, DTM generation and volume calculation in open pit mines, road design and modelling
- DTM and DSM generation in urban areas, automated building extraction, generation of 3-D city models for planning of relay antenna locations in wireless telecommunication, urban planning, microclimate models, propagation of noise and pollutants
- Rapid mapping and damage assessment after natural disasters, e.g., after hurricanes, earthquakes, landslides, etc.
- Measurement of snow- and ice-covered areas, including glacier monitoring
- Measurement of wetlands
- Derivation of vegetation parameters, e.g., tree height, crown diameter, tree density, biomass estimation, determination of forest borders
- Hydrographic surveys in depths up to 70 m.

Other current or possible applications include: landscape design, generation of 3-D models for movie, video and computer-game productions, and computer animation, 3-D models for architectural design and simulation in architectural or civil engineering projects, visualisation and fly- or walk-throughs, plant growth monitoring in precision farming, snow accumulation for avalanche risk estimation, etc.

It is obvious, that ALS is an accurate, fast and versatile measurement technique, which can complement, or partly replace, other existing geo-data acquisition technologies, and open up new exciting areas of application.

Acknowledgements

The authors would like to thank Dr. Chr. Hug for providing some of the figures in this article.

References

Bachman, Chr. G., 1979. Laser Radar Systems and Techniques. Artech House, MA.

Baltsavias, E.P., 1999. Airborne laser scanning: existing systems and firms and other resources. ISPRS Journal of Photogrammetry and Remote Sensing 54 (2–3), 164–198, this issue.

Hug, Ch., 1996. Entwicklung und Erprobung eines abbildenden Laseraltimeters für den Flugeinsatz unter Verwendung des Mehrfrequenz-Phasenvergleichsverfahrens. PhD dissertation, Deutsche Geodätische Kommission bei der Bayerischen Akademie der Wissenschaften, Reihe C, Heft Nr. 457.

Hug, Ch., Wehr, A., 1997. Detecting and identifying topographic objects in imaging laser altimeter data. In: IAPRS, Vol. 32, Part 3–4W2, pp. 19–26.

Jelalian, A.V., 1992. Laser Radar Systems. Artech House, Boston.

Kraus, K., Pfeifer, N., 1998. Determination of terrain models in wooded areas with airborne laser scanner data. ISPRS Journal of Photogrammetry and Remote Sensing 53 (4), 193–203.

Lindenberger, J., 1993. Laser-Profilmessung zur topographischen Geländeaufnahme. PhD dissertation, Deutsche Geodätische Kommission bei der Bayerischen Akademie der Wissenschaften, Reihe C, Heft Nr. 400.

Wehr, A., 1994a. Auslegungskriterien für ein abbildendes CW-Laserentfernungs-meßsystem und seine Realisierung (Teil I). Frequenz 48 (3 to 4), 79–83.

Wehr, A., 1994b. Auslegungskriterien für ein abbildendes CW-Laserentfernungs-meßsystem und seine Realisierung (Teil II). Frequenz 48 (5 to 6), 123–127.

Wolfe, W., Zissis, G., 1978. The Infrared Handbook. Environmental Research Institute of Michigan for the Office of Naval Research, Department of the Navy, Washington, DC.

Young, M., 1986. Optics and Lasers—Series in Optical Sciences. Springer, Berlin, p. 145.